Archives of Materials Science and Engineering

Volume 98
Issue 2
August 2019
Pages 57-67

International Scientific Journal
published monthly by the
World Academy of Materials
and Manufacturing Engineering

DOI: 10.5604/01.3001.0013.4607

Wear resistance of hydrogenated high nitrogen steel at dry and solid state lubricants assistant friction

O.A. Balitskii [a], V.O. Kolesnikov [b,c], A.I. Balitskii [b,d,*]

[a] Ivan Franko National University of Lviv, 50 Drahomanova str., 79005, Lviv, Ukraine
[b] Karpenko Physico-Mechanical Institute National Academy of Sciences of Ukraine, 5 Naukova str., 79060, Lviv, Ukraine
[c] Taras Shevchenko National University of Lugansk, 1 Gogol Sq., 92703, Starobilsk, Ukraine
[d] West Pomeranian University of Technology in Szczecin, 19 Piastow av., 70-310, Szczecin, Poland
* Corresponding e-mail address: balitski@ipm.lviv.ua

ABSTRACT

Purpose: This paper is devoted the investigation hydrogen influence on of wear resistance of high nitrogen steel (HNS) at dry and solid state lubricants assistant friction. It has been established that after hydrogenation at 250 N loading the wear rate increased by 2.9 ... 4.1 times. Microhardness of hydrogenated layer was 7.6 ... 8.2 GPa, that is increased after hydrogenation in two times. After adding the $(GaSe)_xIn_{1-x}$ compounds to the tribo conjugates by X-ray diffraction analysis it has been established the appearance of new phases which formed during the friction process and detected on the friction surface.

Design/methodology/approach: This work presents research results concerning the comparative tests of high nitrogen steels in the circumstances of dry rolling friction. It was conducted the experiments to determine the tribological properties of high-nitrogen steels under rolling friction. The test pieces were manufactured in the form of rollers, and rotated with a linear velocity 2.27 m/s (upper roller), 3.08 m/s (bottom roller). Upper roller is made from HNS was subjected for hydrogenation. Analysis of friction surfaces indicates the complex mechanism of fracture surfaces. The results of the local X-ray analysis and X-ray diffraction analysis has been established the appearance of new phases and elements on the friction surface.

Findings: It has been found that the level of wear resistance of the investigated materials under hydrogenation. Compounds realize chemisorption, tribochemical mechanisms of the formation of thin protective (anti-wear, antifriction) layers on metal surfaces.

Research limitations/implications: An essential problem is the verification of the results obtained using the standard mechanical tests, computer-based image analysis and other methods.

Practical implications: The observed phenomena can be regarded as the basic explanation of reduces the plasticity characteristics after hydrogenation. Applying the $(GaSe)_xIn_{1-x}$ compounds as a lubricant will allow the formation of films on friction surfaces that can minimize surface wear, which will contribute to the transition to a wear-free friction mode. The protective film is a barrier to high shear and normal loads, preserving the base metal of the part and providing reduced wear and friction.

Originality/value: The value of this work is that conducted experiments permit to determine the tribological properties of high nitrogen steels under rolling friction after hydrogenation. After adding $(GaSe)_xIn_{1-x}$ compounds to the tribo conjugates after due to X-ray diffraction analysis it has been established the appearance of new phases which formed during the friction process and detected on the friction surface.

Keywords: Dry friction, Hydrogenated high nitrogen steel, Wear resistance, Embrittlement

Reference to this paper should be given in the following way:

O.A. Balitskii, V.O. Kolesnikov, A.I. Balitskii, Wear resistance of hydrogenated high nitrogen steel at dry and solid state lubricants assistant friction, Archives of Materials Science and Engineering 98/2 (2019) 57-67.

PROPERTIES

1. Introduction

Reducing of oil resource caused for looking of alternative energy fuels, one of which may be a hydrogen. Other problem – looking for new generation of nickel free materials for biomedical application. However, for successful realization of these two tasks we need to use the hydrogen resistant and bio compatible high nitrogen steels HNS [1-7]. Addition of nitrogen to the Cr-Mn steel can significantly increase the mechanical properties. Cold-working stable austenitic steels holds the world record for the yield strength $YS_{0.2}$ = 3400 MPa [3] and can also be widely distributed as tribological materials [4-10]. Hydrogen in steel can be released during the metallurgical processes, as well as from the lubricating, cooling fluid in the process of friction. As a result, we meet the special type of wear - hydrogen wear. For hydrogen wear characterized a high local concentration of hydrogen in the surface layer of steel, which arises due to large temperature gradients, stresses during friction and cause the phenomenon of accumulation and the specific nature of crack growth [11], leading to the complete failure of the layer. Hydrogen wear brings the new ideas on the mechanism of brittle fracture [11-19]. According to the modern classification there are two main types of wear surfaces of steel and cast iron parts under the influence of hydrogen: the dispersion and fracture wear mechanisms [5,6]. The problem arises in the choice of hydrogen resistant steels can be solved by experiment. Preliminary results on the identification of hydrogen degradation, mangan-chromium and nickel-chromium steels has indicate the need to ensure a homogeneous structure of the material for a successful operation in the presence of hydrogen [14-16].

The prospects of nitrogen doping of chromium steels was reported by [17-19], as it reduces the negative nitrogen influence on the hydrogen resistance of the material with high energy packaging, as well as other data on the solubility of the hydrogen mobility and penetration. So with increasing nitrogen content in this steel from 0.077 up to 0.21 mass.% at 573, 773 and 973 K in 1.3-1.45 times decreases the solubility of hydrogen and 2 times – the penetration and diffusion coefficient [15].

2. Materials and test methods

Tribological tests were carried out on a stationary laboratory setup SMT-1 (2070) in the conditions of dry friction. Sliding velocity of the lower roller was 1480 rpm, and the top (made from P900 or DDT 68 steel) – 1240 rpm (slippage was 15%). Lower roller (42 mm) made from steel 45 (1.0503 45/Sk 45 (DIN), 1045) (60 HRC). After heat treatment the substructure was banded and was similar to perlite. The form of the inclusions is the globule. After quenching in water at 850°C troostite was formed along the grain boundaries of austenite (matrix), martensite and retained austenite within the grains. Structure before the examination on the microscope was etched with 3% solution of nitric acid in alcohol, but it is difficult to etch: troostite is etched rapidly and is more etching while martensite still no etching [14]. Top roller was made from high nitrogen steels (chemical composition presented in Table 1). In HNS managed to fix the austenitic microstructure (Fig. 1) (with hardness 4.2...5.0 GPa). The deformation twins nucleate at intersections of active planes and the twin results as product of dislocation reactions among dislocations on these planes [2,4].Manufacturing of high nitrogen steels has made from electrodes melted in electric arc furnaces, which melted to improve the cleanliness at the facility electroslag remealting or electroslag remealting under pressure. After turning blanks samples subjected to diffusion annealing, and further cold hardening. Than the annealing for stress relief and finishing. Cold plastic deformation for these specimens can be up to 60%.

Table 1.
Chemical composition of investigated steels

No.	Alloy	C	Si	Mn	Cr	Ni	Mo	V	N
1.	Alloy (DDT 68) number 1 (upper roller)	0.06	0.52	19.4	17.5	0.13	2.08	0.14	0.97
2.	Alloy number 2 *(bottom roller)	0.42-0.5	0.17-0.37	–	0.25	0.25	–	–	–
3.	Alloy (P 900) number 3 (upper roller)	0.08	0.38	19.0	17.8	1.18	0.13	0.12	0.58

*S up to 0.04%, P up to 0.035, C up to 0.25, Cu up to 0.25, As up to 0.08.

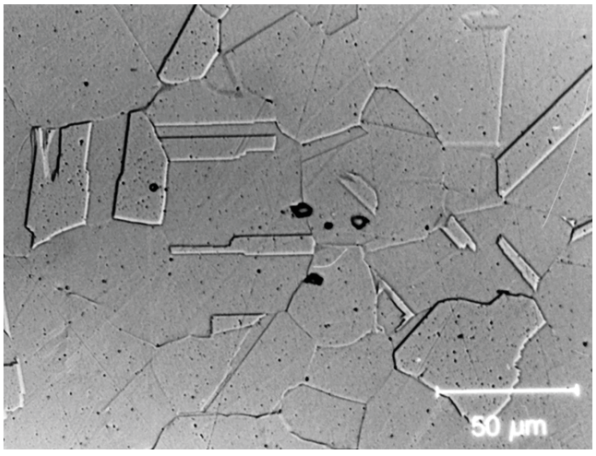

Fig. 1. Microstructure of P900 high nitrogen steel

Linear velocity of the upper roller was 2.27 m/s and the lower 3.08 m/sec. In friction conditions without lubrication the load was 250-600 N. Friction torque was measured in the (N·m), and then for comparison were converted to relative units. Width of the rollers was 1 cm, mass loss of samples was determined by weighing on an analytical balance RADWAG WAA 160 with an accuracy of 0.0001 g, the structure of the steels examined by metallographic, X-ray and electron-microscopic methods of analysis. Structural-phase analysis was performed on a DRON-3 equipment (radiation CuK_{α}). Hydrogenation of alloys was carried out electrolytically with current density 0.5 A/cm^2 in sulfuric acid solution. The wear products investigation was performed using a Neophot 2 microscope with connecting a laptop and a digital camera Canon EOS 30D. This allowed us to determine the size of wear particles and photograph them in various modes of illumination. The friction surface were taken with an electron microscope EVO-40XVP microanalysis system INCA Energy 350. Before the beginning of the tribological experiments it has been performed thorough burn-in samples (with de-oiling of friction surfaces). Burn-in of samples was carried out with the minimum possible load values, with a consequent increase in load to load values corresponding to the beginning of the experiment.

At the same time trying to avoid of the samples overheating.

3. Results and discussions

Figure 2 shows the results of experiments to determine the durability of the samples from steels DDT 68 and 45 (in Table 2 presents some background to the conduct experiments).

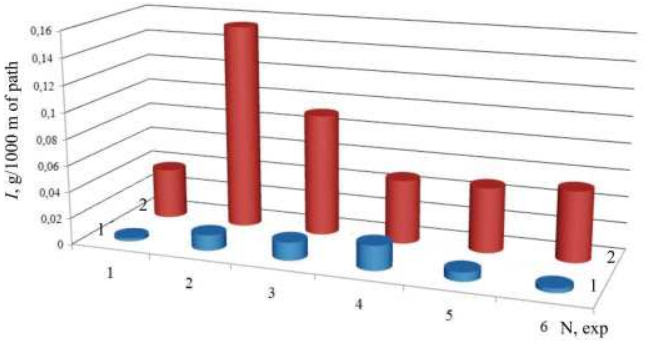

Fig. 2. Results of experiments under dry friction conditions (P = 250 N). The bottom axis number of experiments (№ 1-6). First row number 1 – steel 45, second row number 2 – steel DDT 68

Experiments number 1-6 was conducted sequentially (one after the other). Subsequently there have been several series of experiments, which showed good reproducibility of results and confirmed the identified patterns. Before the experiment number 1 realize the increase in load from 0 to 250 N. Before the experiment number 2 it was realize the clip electrolytic hydrogenation. As result the wear rate increased by 4 times. At a 250 N load the wear rate after hydrogenation increased within 2.9 ... 4.1 times. Figure 3a shows a clip after the experiments. Numeral 1 denotes the lateral surface of the roller, which was mounted a tripod to support roller in sulfuric acid (Fig. 3 shows the appearance of rough gray surface after hydrogenation). Figures 3 and 4 indicate a fundamentally different surface friction on the roller after the experiments.

Table 2.
Explanations for the experiments

Number of experiment	Hydrogenation	Features	Friction torque, %
1	-		100
2	Before the experiment was carried out specimen hydrogenation	There has been a heated surface	155
3	-	Gray hydrogenated layer	111
4	-	Normal friction mode	100-115
5	-	Normal friction mode	100-115
6	-	Surface rasping. Cracks on the side of hydrogenated clip. The experiment was performed 20 hours after hydrogenation	105-116

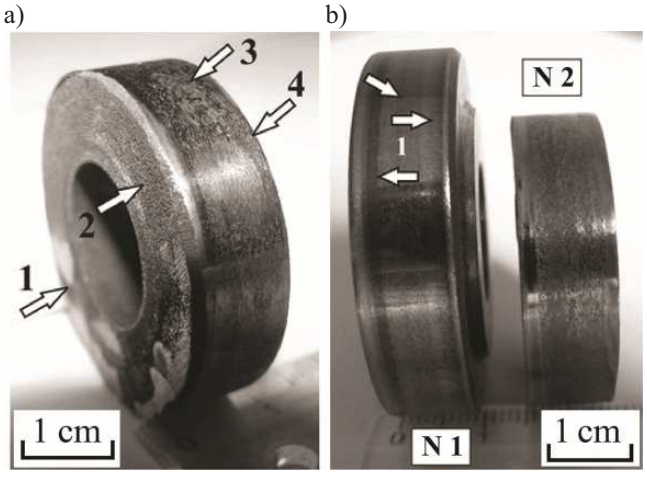

Fig. 3. Clips after the experiments (with hydrogenation): roller from steel, 45 (a), roller from DDT 68 steel (b)

On the surface of the roller (left) (Fig. 4b) shows a gray layer that formed after tribocontact of hydrogenated roller and roller (right), which are not subjected to hydrogenation.

Experiment number 3 data indicate that considerable wear appear in hydrogenated roller. At the same time increase the intensity of hydrogenated clip wear. That may testify about the direct impact of the transport hydrogenated layer on the wear rate. We can assume that hydrogen diffusion take place from hydrogenated roller to non hydrogenated roller and it causes intensification of the destruction of surface layers during the friction process. It is known that hydrogen diffuses very easily under the influence of the temperature gradient in the heated areas of the specimen. The temperature increase recorded during the experiment number 2 on the surface of the conjugate of the bodies also might appear, the reason for which there was an intensification of the destruction of the surface layers of non hydrogenated roller. Experiments

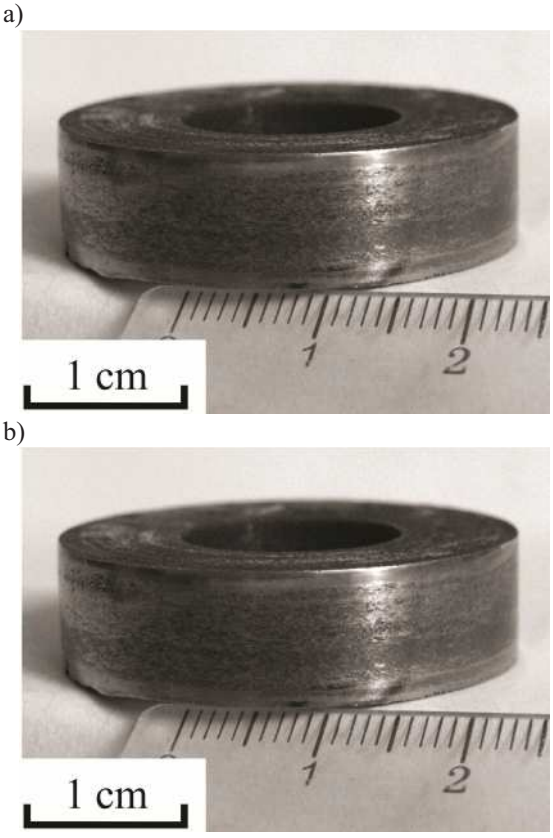

Fig. 4. Rollers after the experiments. Roll from 45 steel type (numeral 1 denotes the occurrence of the gray layer after contact) (a). The surface of roll from high nitrogen steel (b)

number 4-6 show approximately the same stable wear of high nitrogen steel (subjected earlier to hydrogenation) and reduction of wear intensity of roller from 45 steel. Experiment number 6 was performed after 20 hours of roller hydrogenation. Figure 5 shows the high nitrogen

steel surface after hydrogenation and conducting the experiments. On the left from the cavities (Fig. 5) into which the arrow points 1 shows the slip bands which are characteristic for normal wear. Judging by the hydrogenated layer remains (Fig. 5) during the testing process is not all removed, and hence it is firmly rests with the metal surface of the roller. At the same time, the presence of cavities, indicative of the intensification of the surface layer destruction and thus a significant difference in height between the most superior points on the roller surface and the least lowest point.

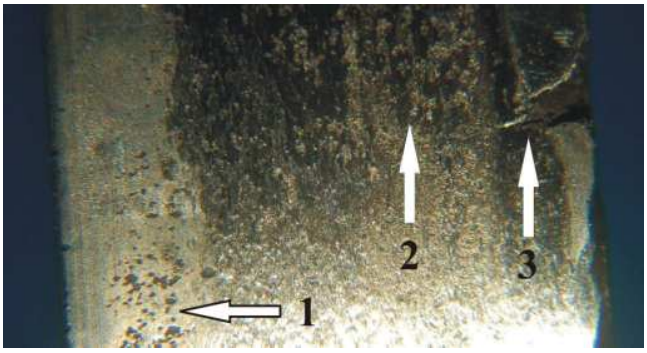

Fig. 5. The surface (x30) of the high nitrogen steel hydrogenated specimen. Numbers denote: 1 – cavity (deepening of which crumble the roller material, 2 – dark hydrogenated layer 3 – crack formed on the roller)

The morphology of wear debris (see Fig. 6) [9,20] has shown stepwise relief with the absence of smooth areas. It was found that the P = 400 N load the average size of wear debris from 25 ... 40 μm and 40 μm ... 100 at P = 500 N.

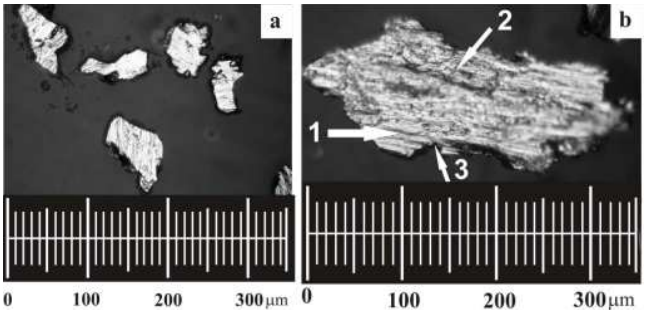

Fig. 6. Wear products before the specimen hydrogenation (a) and the bit of wear hydrogenated layer (b)

Normal friction modes corresponds to the flat shape of wear particles (Fig. 6a). In the hydrogenated samples at P = 250 N the size of particles is equal 350 μm and 600 ... 1000 μm at P = 400 N. Microhardness of hydrogenated layer was 7.6...8.2 GPa that is almost 2 times greater than that of non hydrogenated specimens. In hydrogenated steel at P = 400 N the wear is about 5 times stronger than non-hydrogenated, i.e. with load increases (from P = 250 N) the wear rate increase more than 2.9...4.1 times and increase the sizes of wear particles. In Figure 6b on the particle crumble from the hydrogenated specimen can be observed the step character of the micro relief (position 1). Therefore in this place the pieces of material is separated with higher energy costs according to the brittle mechanism of fracture. Zone 2 indicates the occurrence of intense heat processes followed by gripping and pulling out of material. Arrow 3 shows the presence of cracks on the particle of wear.

Figure 7 shows the high nitrogen steel friction surface. In the initial stages of friction non hydrogenated steel have micro surface slip bands (Fig. 7a, position 1). Hydrogenated specimens are destroyed more rapidly and the friction surface of the specimens differ significantly from non hydrogenated. Position 1 on Fig. 7b indicates furrow microrelief. Position 2 and the white dotted lines delineate the area around the most typical for this type of fracture, which arise after the destruction of hydrogenated area. Position 3 indicates a significant depression, resulting from spalling and separation of large fragments of material. Position 4 indicates a significant area in the zone devastated by severe plastic deformation (micro step), and thermal processes of setting, which differs significantly from zone 2.

It has been established experimentally that for heavy-duty friction maximum temperature is not formed on the surface but at a certain depth. This creates conditions in which hydrogen (if it is adsorbed on the surface of the part) under the influence of the temperature gradient diffuses into the surface. It is concentrated and causes embrittlement of the surface layers, consequently increases the wear.

The results of local analysis shows that on the surface of the roller is fixed oxygen (up to 8.4 wt. %) (Fig. 8). It is a kind of wear as oxidative form of wear [20], as a result of which fracture processes are smoothed out and the flow is not as strong as the oxidative form of wear but accompanied by the formation of secondary structures on the surface friction. The presence of oxygen on the surface of the samples may also indicate the formation of oxides, i.e. intensive processes of destruction that occur on the surface of the roller. May be they take a role of catalyst to the formation of secondary structures on the friction surface. Previously observed phenomenon [20] the steel ability to hold for a long time on the friction surface residues of the film from the lubricant or may also contribute to the formation of oxides on the surface (for example, Fe_2O_3 and

Fe_2O_4). According to electron diffraction data [20] the secondary structure are the ferrous oxides, which is the most common compound of non stoichiometric composition having a sufficiently wide homogeneity $Fe_{1-x}0$ field. In the equilibrium conditions these compound is formed only at temperatures above 570°C, while at more low temperatures it is unstable and decays due to the reaction $4Fe0 \rightarrow Fe_30_4 + Fe$. Space technology needs the use of new lubricants. In a deep vacuum, the exposed surfaces of the bodies are degassed, and the lubricant and other coatings evaporate, the friction coefficient between the surfaces increases significantly, as a result of which cold welding is possible.

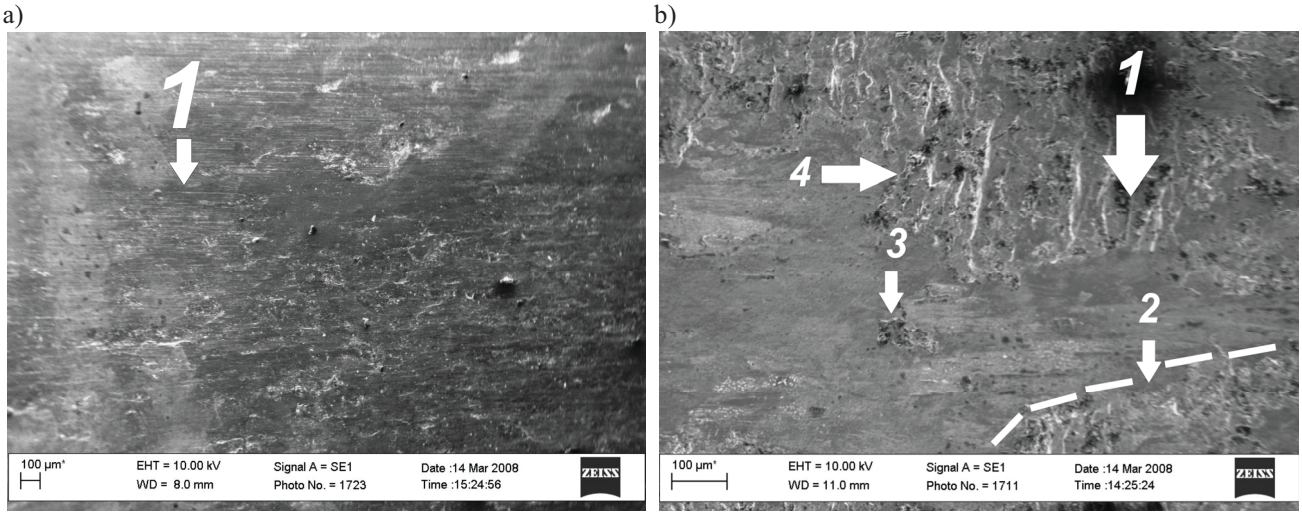

Fig. 7. The friction surface of high nitrogen steel: start of tribological tests before hydrogenation (a), after hydrogenation – the initial test before the catastrophic wear (b)

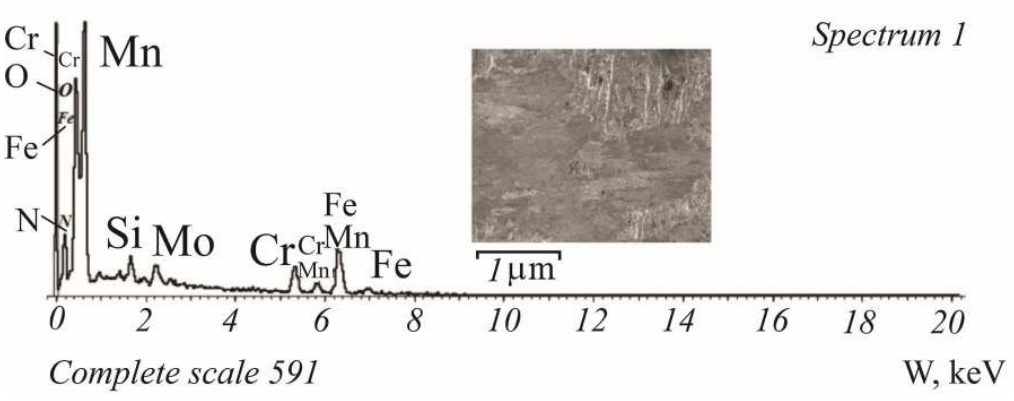

Fig. 8. The results of X-ray investigation of high nitrogen steel chemical composition

Take to account that vacuum exposes rubbing surfaces, then it is important for materials to have a high degree of adhesive component. An abnormally high ability of high nitrogen manganese steels was revealed under conditions of "oil starvation" to hold a layer of lubricant residues on its surface [20]. It is known that when graphite hits between friction surfaces, the wear rate decreases [22]. This is due to the layered structure of graphite. However, the use of graphite as a pure lubricant is a complicated procedure due to the large losses of graphite itself and the fragility of the lubricating effect of this material, which necessitates the periodic replenishment of graphite tribo-conjugation. Graphite is used as a lubricant in a vacuum, because its ability depends on adsorbed moisture, which is completely removed in a vacuum. The lubricity of graphite depends on the presence of an oxide film on the surface. Molybdenum disulfide is also not stable in vacuum. $CrSe_2$, $MoSe_2$, WSe_2, VSe_2, $NbSe_2$, $TaSe_2$, $TiSe_2$, $ZrSe_2$, $HfSe_2$,

$ReSe_2$, $ThSe_2$ and USe_2 concidered as solid state lubricant [20-27]. Selenides $MoSe_2$, WSe_2, NbSe are successfully used as ingredients of self-lubricating materials designed for friction in ultra-high vacuum [20-27]. Compounds of $A^{III}B^{VI}$ type having a layered structure can be also used as a lubricant. In particular, these compounds include: InSe, GaSe, GaTe, (GaSe)In, MoSe, MoS, WSe, WS_2.

The wear rate at a load of 25 kg for steel P900 was 0.1656 g/1000 meters of path (m. p.), for steel 1.0503 0.1973 g/1000 m. p. coefficient of friction is 0.96. After adding the $(GaSe)_{0.75}In_{0.25}$ powder, the friction coefficient decreased to 0.4, and the wear rate of P900 was 0.005799 g/1000 m. p., steel 1.0503-0.00328 g/1000 m. p. The results of the second experiment: P900 – 0.006579 g/1000 m. p., steel 1.0503-0.006579 g/1000 m. p. The test duration was 3 minutes. After supplying $(GaSe)_{0.X}In_{0.X}$ compounds to the tribo conjugation (by the scheme presented in Fig. 9), the wear rate sharply decreased. The film first appeared and was held on austenitic manganese steel. The appearance of the film on austenitic manganese steel and steel 1.0503 is different.

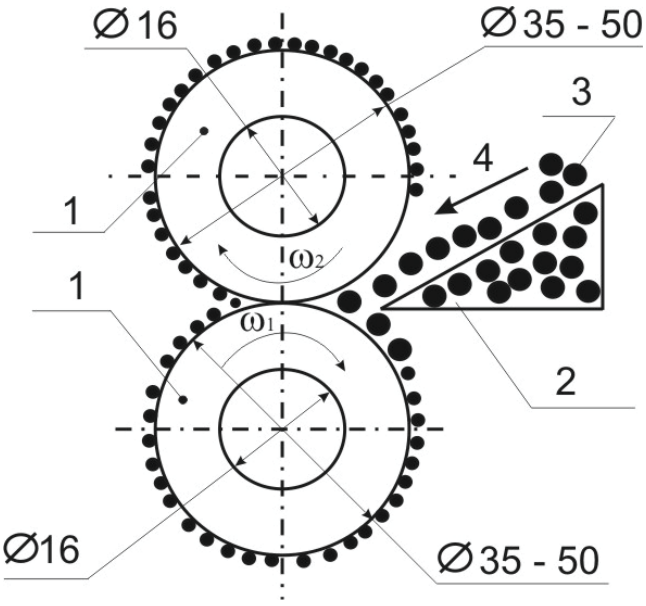

Fig. 9. Testing scheme and sample sizes: 1 – roller; 2 – a device for uniform supply of compounds of $A^{III}B^{VI}$ type; 3 – lubricant (compounds of $A^{III}B^{VI}$ type); 4 – direction of supply of $A^{III}B^{VI}$ compounds type [20]

On the surface of the P900 steel (similar to hydrogen degradation process [28]) rollers, a continuous film of a dark violet matte shade was formed (Fig. 10c), and on the 1.0503 steel (Figs. 10a,b) it was black. After 20 minutes of continuous testing (for P900 this is 2.490 m. p.), the film formed on the surface completely merges with the surface of the P900 steel. And on steel 1.0503 (4830 m. p.), the film began to lag (blisters and bubbles appeared), burrs appeared on the surface end (Fig. 10a). When graphite was added to the friction pair, the friction coefficient was 0.45, i.e. was greater than with friction with $(GaSe)_{0.75}In_{0.25}$ (Fig. 11).

Then $(GaSe)_{0.25}In_{0.75}$ was supplied to the tribo conjugation. The wear of P900 steel was 0.009129 g/1000 m. p. Steel 1.0503 respectively 0.0039124 g/1000 m. p. (the results of experiments on mass loss are summarized in Figure 11).

The wear of these steels under dry friction conditions showed their high wear resistance compared to conventional steels. This is due to the fact that these materials have high physical and mechanical properties. The nature of manganese austenite allows these steels in conditions of dry friction have a high bearing capacity in comparison with conventional materials. However, it is possible to significantly change their operational properties by conducting heat treatment and complex technological cycles (which include long-term forging, rolling, rough rolling, cold stretching.

The low friction coefficients (0.4) of $(GaSe)_{0.25}In_{0.75}$ powder are due to the large size of the metal atoms, as a result of which the Van der Waals forces are weakened and the simple structure is more easily split. There is a strong chemical bond between the metal and Se atoms, and this bond is weak between the Se atoms. Therefore, a shift with little friction occurs in the direction of bonds between Se atoms, which ensures high lubricating properties. Reducing the load from 25 to 10 kg is accompanied by a significant decrease in the wear rate, as well as the values of the friction coefficients (by an order of magnitude). The friction coefficients obtained during testing in a nitrogen atmosphere at 70°C and a sliding speed of 1.1 m/s at a pressure of 10.5 kg/cm^2 are: $MoSe_2$ – 0.02; WSe_2 – 0.02; NbSe – 0.06; $MoSe_2$ – 0.03. The friction coefficients for steels and cast irons at specific pressure in similar conditions are 0.4-0.8, i.e. more than with lubrication $(GaSe)_xIn_{1-x}$ [22]. When compound $(GaSe)_{0.25}In_{0.75}$ was added to tribological conjugation, the appearance of new phases (formed during the friction process) was detected on the friction surface of both steels by X-ray diffraction analysis (Fig. 12). On the 1.0503 steel surface GaSe disappears under friction conditions and passes into a new phase. The presence of oxygen in the atmosphere promotes the formation of (In_2O_3) and (In_2O_3) oxides [20].

The vertical lines show the positions of the Bragg imprints of the composite phases: $In_{1-x}Ga_x$ (above) and $Ga_{1-x}In_xSe$ (below) X_1 and X_2 new phases formed after friction.

a)

b)

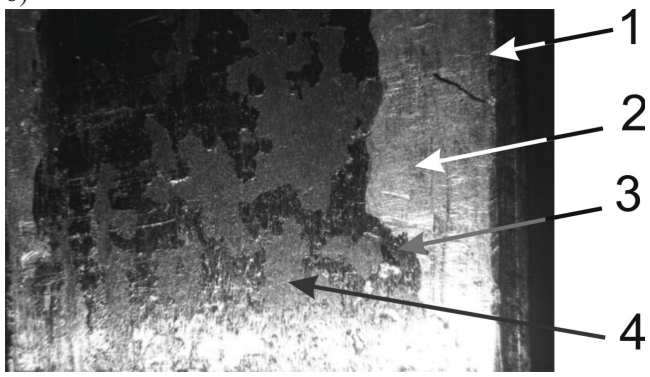

c)

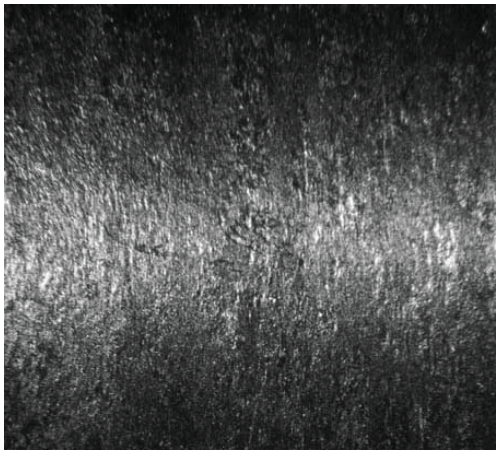

Fig. 10. Surface of steel 1.0503 after 20 minutes of continuous testing (the black colour of the film is visible along with the swellings), the burrs along the edge of the roller are (a). 1 – steel surface (1.0503) in the edge of the roller; 2 – the surface of the roller from which the film disappeared; 3 – the film (type 1), which formed during friction upon the addition of $(GaSe)_{0.25}In_{0.75}$; 4 – a film (type 2), which formed during friction upon the addition of $(GaSe)_{0.25}In_{0.75}$; (magnification × 18) (b); P900 steel surfaces (c)

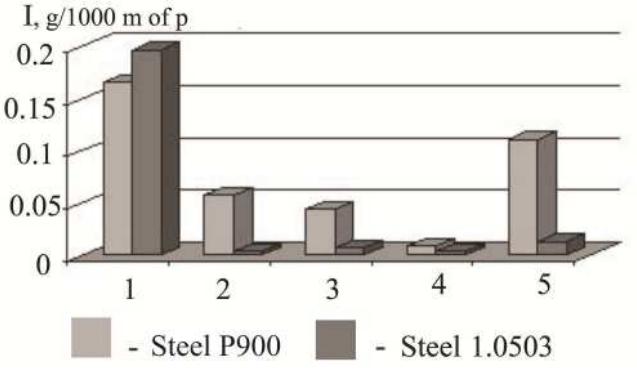

Fig. 11. The diagram of comparative wear of steels under different conditions of the experiment: 1 – dry friction; 2 – experiment No. 1 – friction with the addition of $(GaSe)_{0.75}In_{0.25}$; 3 – experiment No 2 – friction with the addition of $(GaSe)_{0.75}In_{0.25}$; 4 – friction upon addition of $(GaSe)_{0.25}In_{0.75}$; 5 – friction after graphite adding

Hugo M. Rietveld refinement of X-ray diffraction analysis for these materials can established next issues: the $In_{1-x}Ga_x$ phase (solid solution of Ga in In) contains about 40 wt. % and represents a tetragonal structure(belongs to the space group I4/mmm). The period of the crystal lattice: a = 3.2490 Å; c = 4.9467 Å. For comparison, pure In: I4/mmm; a = 3.2542 Å; c = 4.9542 Å. The $Ga_{1-x}In_xSe$ phase (x>0.2) (GaSe structural type) ~ 60% of the mass has a hexagonal structure and belongs to the P-6 space group. The periods of the crystal lattice: a = 3.8311 Å; c = 16.2443 Å. For comparison, pure GaSe: a = 3.7421 Å; c = 15.9193 Å, $Ga_{0.8}In_{0.2}Se$ phase: a = 3.801 Å; c = 16.12 Å. Factor of divergence (disagreement) of the refinement: Rp = 7.82%.

The composition of the new phase includes metal. It is known that a characteristic feature of the chalcogenides of Ti, V, Cr, Mn, Fe, Co and Ni has the tendency of cations and vacancies to be located in octahedral locations. As a result of this, many compounds with the vacant structure arise in the region of homogeneity. The formation and existence of compounds of variable composition depends on temperature. If we take into account that elevated temperatures arise on the friction surfaces in tribological conjugation, then together with contact pressures they also contribute to the formation of new phases. It is known that the selenium atom in the isolated state has the s^2p^4 valence electron configuration, which is prone to completion due to the electrons of other elements with which it reacts, as well as the selenium itself to the stable d^5 - s^2p^6 configuration. Naturally, the loss of electrons by the selenium atom is also possible with their transfer to the metal atom. Selenides of d - transition metals are heterodesmic compounds [20]; they are characterized by a covalent metal type of bond with the application of a certain fraction of the ionic bond.

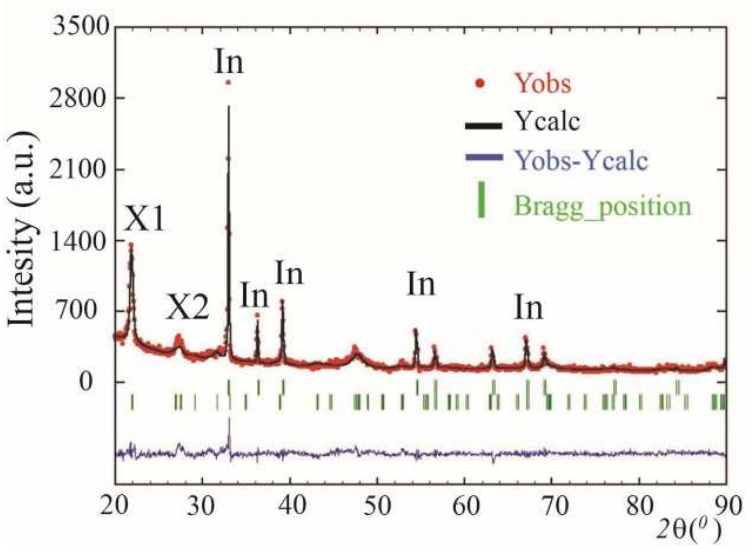

Fig. 12. X-ray difracrogramms [20] taken after friction tests from the 1.0503 steel surface. Experimental (♦), calculated (solid line above) and difference (below) profiles of X-ray diffraction of the $(GaSe)_{0.25}In_{0.75}$ alloy

The formation of a layered structure in compounds of this type can be explained by the fact that within the individual layers formed by both metal and non-metal atoms, predominantly strongly covalent bonds arise, and the bond between the individual layers is carried out by non-localized electrons and is metallic in nature [20]. The strength of the interlayer bond will depend on the degree of delocalization of electrons in the crystal lattice of the compound, which is manifested in the degree of "metallicity" of the substance. It is well known that selective transfer of substances can occur in tribological conjugation and the regime of structural adaptability is carried out, as a result of which structures are formed on the friction surfaces that are capable of supporting a wear-free friction mode [20]. Also, great opportunities open up for the use of additives in oils. The introduction of these components into the oil increases the strength of the oil film and slows down the process of its destruction in the friction zone. Active components and nanoscale processes (intercalation) form a self-healing thin protective film on the friction surfaces. The structural features of layered structures of type $A^{III}B^{VI}$ (weak Van der Waals bond between layers) allow the introduction of foreign atoms or molecules into the interlayer space. X-ray diffraction analysis recorded a change in the crystal lattice parameters for the $Ga_{1-x}In_xSe$ phase. A "weak" Van der Waals physical interaction with a closer approximation of molecules can go into a chemical bond. Between these types of interaction there is a quantitative (in terms of the binding energy) and qualitative difference. For physical interaction, the binding energy is 0.05-0.1 eV, and for chemical adsorption, 1-8 eV [20]. The first type of interaction is universal, the second is selective. During physical interaction, the structure of the electron shells does not change, just as the nature of the distribution of electron density in a solid does not change. During chemisorption the electron shells of adsorbed atoms change and the electron density in the surface layer of a solid changes noticeably [20]. Graphite lubricants are of limited use due to their inability to maintain lubricating properties in vacuum or in moist air due to an increase in the friction coefficient under loads increasing. Therefore, the use of Se-type $A^{III}B^{VI}$ compounds with a layered structure as a lubricant can have wide possibilities.

4. Conclusions

It was conducted the experiments to determine the tribological properties of high-nitrogen steels under rolling friction.

The test pieces were manufactured in the form of rollers, and rotated with a linear velocity 2.27 m/s (upper roller), 3.08 m/s (bottom roller). Upper roller is made from HNS was subjected for hydrogenation. As a result at 250 N loading the wear rate increased by 2.9 ... 4.1 times. Microhardness of hydrogenated layer was 7.6 ... 8.2 GPa, that is increased after hydrogenation in two times. Analysis of friction surfaces indicates the complex mechanism of fracture surfaces.

The results of the local X-ray analysis showed the presence of oxygen on the friction surface. It is obvious that oxygen is part of the oxides formed under intense heat setting. After adding $(GaSe)_xIn_{1-x}$ compounds to the tribo conjugates after X-ray diffraction analysis it has been established the appearance of new phases which formed during the friction process and detected on the friction surface. Compounds realize chemisorption, tribochemical mechanisms of the formation of thin protective (anti-wear, anti-friction) layers on metal surfaces. Applying the $(GaSe)_xIn_{1-x}$ compounds as a lubricant will allow the formation of films on friction surfaces that can minimize surface wear, which will contribute to the transition to a wear-free friction mode. The protective film is a barrier to high shear and normal loads, preserving the base metal of the part and providing reduced wear and friction.

References

[1] F.O. Nestle, H. Speidel, M.O. Speidel, High nickel release from 1- and 2-euro coins, Nature 419 (2002) 132, DOI: https://doi.org/10.1038/419132a.

[2] M.O. Speidel, From High-Nitrogen Steels (HNS) to High-Interstitial Alloys (HIA), in: M.O. Speidel (Ed.), HNS 2003: High Nitrogen Steels, Hochschulverlag AG an der ETH Zürich,2003, 1-8.

[3] A.I. Balitskii, O.V. Machnenko, O.A. Balitskii, V.A. Grabovskii, D.M. Zaverbnii, B.T. Timofeev, Fracture mechanics and strength of materials: Reference book, V.V. Panasyuk (Editor-in-chief), V.8. Strength of materials and durability of structural elements of nuclear power plants, A.I. Balitskii (Ed.), PH "Akademperiodyka", Kyiv, 2005, 544.

[4] P.J. Uggowitzer, R. Magdowski, M.O. Speidel, High nitrogen austenitic stainless steels – properties and new developments, La Metallurgia Italiana 86/6-7 (1994) 347-354.

[5] J. Romu, J. Tervo, H. Hännien, J. Liimatainen, Wear resistance of high nitrogen austenitic stainless steels manufactured by molten and powder metallurgy routes, Proceedings of the 3rd International Conference High nitrogen steels "HNS 93", Kiev, Ukraine, 1993, 372-378.

[6] R. Büscher, A. Fischer, Tribological performance of austenitic high-nitrogen steels for biomedical applications, Steel Grips, High Nitrogen Steels 2 (2004) 481-491.

[7] N. Efros, L. Korshunov, B. Efros, N. Chernenko, L. Loladze, Nanostructure and tribological properties of nitrogen-containing Fe-Mn-Cr alloys upon friction and abrasive action, Steel Grips, High Nitrogen Steels 2 (2004) 391-395.

[8] M. Diener, Application of High Nitrogen Steels for Rail Wheels, Proceedings of the 2nd International Conference of High Nitrogen Steels, Aahen, Germany, 1990, 405-410.

[9] O.I. Balyts'kyi, V.O. Kolesnikov, P. Kawiak, Tribo-engineering properties of austenitic manganese steels and cast-irons under the conditions of sliding friction, Materials Science 41/5 (2005) 624-630, DOI: https://doi.org/10.1007/s11003-006-0023-7.

[10] U.I. Thomann, P.J. Uggowitzer, Wear-corrosion behaviour of biocompatible austenitic stainless steels, Wear 239/1 (2000) 48-58, DOI: https://doi.org/10.1016/S0043-1648(99)00372-5.

[11] I. Dmytrakh, Corrosion fracture of structural metallic materials, Effect of electrochemical conditions in crack, Strain: An International Journal for Experimental Mechanics 47/2 (2011) 427-435, DOI: https://doi.org/10.1111/j.1475-1305.2010.00784.x.

[12] T. Michler, J. Naumann, Hydrogen environment embrittlement of austenitic stainless steels at low temperatures, International Journal of Hydrogen Energy 33/8 (2008) 2111-2122, DOI: https://doi.org/10.1016/j.ijhydene.2008.02.021.

[13] T. Michler, J. Naumann, Hydrogen environment of Cr-Mn-N-austenitic stainless steels, International Journal of Hydrogen Energy 35/3 (2010) 1485-1492, DOI: https://doi.org/10.1016/j.ijhydene.2009.10.050.

[14] O.I. Balyts'kyi, L.M Ivaskevich, V.M. Mochulskyi, O.M. Holiyan, Influence of hydrogen on the crack resistance of 10Kh15N27T3V2MR steel, Materials Science 45/2 (2009) 258-267, DOI: https://doi.org/10.1007/s11003-009-9184-5.

[15] A.I. Balitskii, L.M. Ivaskevich, V.M. Mochulskyi, Crack resistance of age-hardening Fe-Ni alloys in gaseous hydrogen, Proceedings of the 18th European Conference on Fracture, Fracture of Materials and Structures from Micro to Macro Scale, Dresden, Germany, 2010, Paper N 80, 1-8.

[16] T. Michler, J. Naumann, E. Sattler, Influence of high pressure gaseous hydrogen on S–N fatigue in two austenitic stainless steels, International Journal of Fatigue 51 (2013) 1-7, DOI: https://doi.org/10.1016/j.ijfatigue.2013.01.010.

[17] T. Michler, J. Naumann, M.P. Balogh, Hygrogen environment embrittlement of solution treated Fe-Cr-Ni, Materials Science and Engineering: A 607 (2014) 71-80, DOI: https://doi.org/10.1016/j.msea.2014.03.134.

[18] T. Michler, J. Naumann, Microstructural aspects upon hydrogen environment embrittlement of various bcc

steels, International Journal of Hydrogen Energy 35/2 (2010) 821-832, DOI: https://doi.org/10.1016/j.ijhydene.2009.10.092.

[19] T. Michler, M. Linder, U. Eberle, J. Meusinger, Assessing hydrogen embrittlement in automotive hydrogen tanks, in: R.P. Gangloff, B.P. Somerday (Eds.), Gaseous Hydrogen Embrittlement of Materials in Energy Technologies. The Problem, its Characterisation and Effects on Particular Alloy Classes, Woodhead Publishing Limited, 2012, 94-125, DOI: https://doi.org/10.1533/9780857093899.1.94.

[20] A.A. Balitskii, V.A. Kolesnikov, O.B. Vus, Tribotechnical properties of nitrogen manganese steels under rolling friction at addition of $(GaSe)_xIn_{1-x}$ powders into contact zone, Metallofizika i Noveishie Tekhnologii 32/5 (2010) 685-695.

[21] K.H. Hu, J. Wang, S. Scharaube, Y.F. Xu, X.G. Hu, R. Stengler, Tribological properties of MoS_2 nanoballs as filler in polyoxymethylene-based composite layer of three-layer self-lubrication bearing materials, Wear 266/11-12 (2009) 1198-1207, DOI: https://doi.org/10.1016/j.wear.2009.03.036.

[22] R. Tenne, L. Margulis, M. Genut, G. Hodes, Polyhedral and cylindrical structures of tungsten disulphide, Nature 360 (1992) 444-446, DOI: https://doi.org/10.1038/360444a0.

[23] V. Pettarrin, M.J. Churruca, D. Felhos, J. Karger-Kocsis, P.M. Frontini, Changes in tribological performance of high molecular weight high density polyethylene induced by the addition of molybdenum disulphide particles, Wear 269/1-2 (2010) 31-45, DOI: https://doi.org/10.1016/j.wear.2010.03.006.

[24] A. Adebogun, R. Hudson, A. Breakspear, C. Warrens, A. Gholinia, A. Mattehews, P. Withers, Industrial Gear Oils: Tribological Performance and Subsurface Changes, Tribology Letters 66:65 (2018) 1-13, DOI: https://doi.org/10.1007/s11249-018-1013-2.

[25] D. Klammann, Lubricants and related products (Synthesis properties applications international standards), Verlag Chemie GmbH, D-6940 Weinheim, 1984, 488.

[26] S. Bistac, A. Galliano, Nano and macro tribology of elastomers, Tribology Letters 18/1 (2005) 21-25, DOI: https://doi.org/10.1007/s11249-004-1701-y.

[27] L. Rapoport, Yu. Bilik, Y. Feldman, M. Homyofer, S.R. Cohen, R. Tenne, Hollow nanoparticles of WS_2 as potential solid-state lubricants, Nature 387 (1997) 791-793, DOI: https://doi.org/10.1038/42910.

[28] A.I. Balitskii, V.V. Panasyuk, Workability assessment of structural steels of power plant units in hydrogen environments, Strength of Materials 41/1 (2009) 52-57, DOI: https://doi.org/10.1007/s11223-009-9097-4.